N-caprylammonium chloride: a solid membrane model

ARTICLE *in* THE JOURNAL OF PHYSICAL CHEMISTRY · JUNE 1992

Impact Factor: 2.78 · DOI: 10.1021/j100192a064

6 AUTHORS, INCLUDING:

Kurt Schenk

École Polytechnique Fédérale de Lausanne

239 PUBLICATIONS **2,979** CITATIONS

SEE PROFILE

Craig Alan Ogle

University of North Carolina at Charlotte

84 PUBLICATIONS **1,415** CITATIONS

SEE PROFILE

Gervais Chapuis

École Polytechnique Fédérale de Lausanne

397 PUBLICATIONS **4,036** CITATIONS

SEE PROFILE

n-Caprylammonium Chloride: A Solid Membrane Model

K. J. Schenk,[†,‡] C. A. Ogle,[§] D. Schwarzenbach,[‡] G. Chapuis,[‡] J.-C. Cornut,[†] and M. Rey-Lafon*[,†]

Laboratoire de spectroscopie moléculaire et cristalline, U.R.A. 124, Université de Bordeaux I, 351, cours de la Libération, F-33405 Talence, France; Institut de cristallographie, Université de Lausanne, BSP Dorigny, CH-1015 Lausanne, Switzerland; and Department of Chemistry, University of North Carolina at Charlotte, Charlotte, North Carolina 28223 *(Received: January 10, 1992)*

n-Caprylammonium chloride (C8Cl) undergoes three thermotropic phase transitions between 304 and 311 K. Its high-temperature phases (β, γ, and α) are very disordered and resemble smectic mesophases found in biomembranes. The δ-phase (stable between 278 and 304 K) of C8Cl is studied by means of single-crystal X-ray diffraction. Chlorine and nitrogen atoms form a 3-periodic arrangement, but the carbon atoms oscillate about the long axes of the *n*-caprylammonium chains. These exist as several conformers which can be approximated as a single, entirely extended chain. The cell of the δ-phase allowed us to index powder X-ray photographs of the other phases of C8Cl and to deduce a structural description for them. Percentages of conformers, G forms, and GTG′/GTG sequences in the various phases are estimated from the analysis of characteristic IR and Raman bands, especially of the ω-bideuterated derivative. By a combination of our conclusions with previous NQR and NMR results, a rather complete picture of the phase transitions is deduced: they are brought about by the disordering of the aliphatic chains on one hand and of the hydrogen bonding scheme at the Cl–N interface on the other hand. The dynamics of these two subsystems behave quite differently indeed: changes in the chains occur very gradually, whereas variations in the interface happen quite abruptly. C8Cl successfully mimics the temperature dependence of the bilayer thickness, chain cross section, and order as well as the chain separation/interdigitation transition in biological membranes.

Introduction

Pure, crystalline phases of membrane lipids such as lecithins, sphingolipids, or cholesterol derivatives have been known to constitute useful model systems for biological membranes for a long time. An ever increasing number of such structures at room temperature is being published. But few, if any, disordered structures of the corresponding high-temperature phases have been determined. In this investigation we use X-ray diffraction and vibrational spectroscopy to deduce a rather detailed description of the high-temperature phases (β, γ, and α) of *n*-caprylammonium chloride (C8Cl). This compound has been raising considerable interest in the past few years due to its many phase transitions[2-4] and the suspected occurrence of a chain separation $\rightleftharpoons$ interdigitation transition.[1,8]

The crystallization of the noninterdigitated phases of *n*-alkylammonium chlorides (dubbed CnCl) represents a justly feared Sisyphean task. Their lack of order and strong intermolecular forces usually reduces any growth attempt to the luckless secretion of semiamorphous, soapy aggregates of grains infested with defects of all kinds. In fact, it is even difficult to obtain a well-defined powder of these phases (Figure 1).

Naturally, the knowledge of their structures is of prime importance for the interpretation of the thermotropic phase transformations in CnCl. The value of just knowing the unit cell has recently been demonstrated by the example of C10Cl.[1] In this system, powder diagrams could be successfully indexed, based on the unit cell of phase δ[8]. (This notation refers to phase δ of C8Cl.)

The potential usefulness of the structure of C8Cl for interpreting the phase transitions in the CnCl becomes evident in the light of the following analogies between the CnCl: (i) DSC experiments[2-4] reveal a comparable sequence of phases with analogous enthalpies at corresponding transitions. (ii) Powder diagrams of corresponding phases can be indexed in similar cells: we call such phases "isomorphous".[1] (iii) ^{14}N,^{35}Cl NQR spectroscopy[5,6] yields the same number of chemically equivalent nitrogen and chlorine atoms with comparable field gradients and asymmetry parameters in corresponding phases. (iv) ^1H NMR spectroscopy[7,8] detects rather similar proton second moments in homologous phases.

Undoubtedly, the structure of one of the noninterdigitated phases of the CnCl would considerably advance the understanding of their microscopic transition mechanisms. Phase δ[8] is the sole of the noninterdigitated phases that is stable at room temperature. In view of the destructive nature of the phase transitions in the CnCl and the experimental difficulties of high- and low-temperature studies, phase δ[8] is the best candidate for a structure determination.

A proton second moment of 5 G (ref 2) certainly indicates a state of the aliphatic chains closer to a liquid than to a well-ordered, closely packed solid. Clearly, this chain disorder will thwart a routine X-ray structure determination. But the recent implementation of soft constraints[9] into our least-squares program allowed us to hope to tackle the disorder problem successfully.

Indeed, we were able to refine a rather convincing static model for the structure. Of course, it did not reach the usual precision one is accustomed to from X-ray work, but the resulting structure description satisfied most of the physical and chemical reasonableness criteria.

But it was also clear that X-ray diffraction alone could not provide answers to all open questions, in particular to those regarding the conformations of the alkylammonium chains in the disordered phases. To complement the X-ray investigation, we undertook a vibrational spectroscopy study. Indeed, the combination of the two techniques results in a rather satisfactory picture of the thermotropic phase transitions in C8Cl.

Experimental Details

Synthesis of *n*-Octylammonium Chloride (C8Cl). Hydrochloric acid was added to an alcoholic solution of *n*-octylamine (Fluka, purer than 99%, by GC). The resulting white precipitate is only very slightly hygroscopic. It needed no further purification since it melts (heating rate 1 °C min^{-1}) at 476 K, which seemed close enough to the literature value[2] of 477 K.

Preparation of 7,7-Dideuteriooctylammonium Chloride (DωC8Cl). Acetic anhydride, 1,5-dibromopentane, phosphorus tribromide, HMPA, NaCN, CuCN, $LiAlH_4$, and $LiAlD_4$ were used as obtained from Aldrich Chemical Co. THF and ether were distilled from sodium benzophenone just prior to use. DMSO was vacuum distilled and stored over molecular sieves. The purity of each intermediate was established by comparison to commercial undeuterated products using gas chromatography on a SP2100 column.

1,1-Dideuterioethanol. In a round-bottom flask, charged with nitrogen and equipped with an addition funnel, a reflux condenser, and a magnetic stirbar, $LiAlH_4$ (5.0 g, 0.12 mol) and 250 mL of ether were stirred while the acetic anhydride solution (20 mL, 0.21 mol; in 50 mL of ether) was added dropwise. After the

[†] Université de Bordeaux I.
[‡] Université de Lausanne.
[§] University of North Carolina.

0022-3654/92/2096-5530$03.00/0

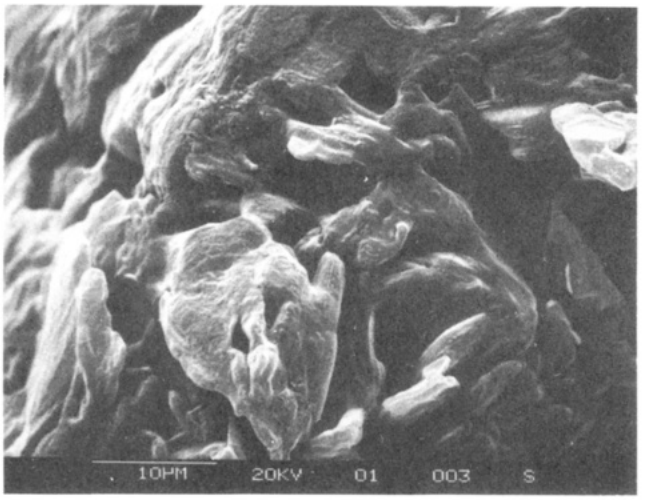

Figure 1. Electron micrograph of a typical "powder" sample of C8Cl.

addition had been finished, the suspension was refluxed for 1 h. After this cooled to room temperature, sequentially, 5 mL of water, 5 mL of 15% aqueous NaOH, and 15 mL of water were added. The white salts were removed by filtration. The ether and the deuterated alcohol (13 g, 80%) were separated by fractional distillation.

1,1-Dideuteriobromoethane. The alcohol above (13 g) was added dropwise to a stirred excess of PBr_3 (32 mL, 0.34 mol) in a round-bottom flask with a condenser. Upon completion of the alcohol addition, the mixture was allowed to stir overnight. The condenser and dropping funnel were removed and replaced by a distillation head and condenser and receiving flask. The bromide (21.8 g, 58% yield) was distilled from the phosphorus residue and washed with water to remove any dissolved HBr and starting alcohol.

6,6-Dideuterio-1-bromoheptane. A solution of the Grignard reagent from the alkyl bromide above was prepared by slow addition of the bromide (20 g, 0.18 mol; in 15 mL of THF) to an excess of stirred magnesium (6.0 g, 0.25 mol) in 75 mL of THF. A crystal of iodine was added to initiate the reaction. The solution was refluxed for 1 h after the addition had been completed. The Grignard reagent was allowed to cool to room temperature. The solution was rapidly added via syringe to a stirred suspension of CuCN (17.7 g, 0.18 mol), 1,5-dibromopentane (36.8 mL, 0.27 mol), and HMPA (10 mL) in 150 mL of THF. The suspension was allowed to stir for 1 h before workup. Ether (200 mL) was added to the solution which was then washed with water five times to remove the salts and the HMPA. The organic phase was dried and the solvent was removed by rotary evaporation, leaving the desired compound, the starting dibromide, and tetradeuteriononane. No attempts were made to separate the mixture.

6,6-Dideuterio-1-cyanoheptane. Sodium cyanide (11.9 g, 0.27 mol) was dissolved in 100 mL of DMSO; heating was required to complete dissolution. The crude bromide was then added. After the initial exotherm had subsided, the flask was warmed to 80 °C for 2 h and then allowed to cool to room temperature. Ether (200 mL) was added. The mixture was then washed five times with water to remove the DMSO and 1,5-dicyanopentane. The organic phase was dried, and the solvent was removed by rotary evaporation. The residue was shown to be cyanoheptane and nonane by gas chromatography. No attempts were made to further purify the product.

6,6-Dideuterio-1-aminooctane. The mixture above was dissolved in 20 mL of ether and added dropwise to a stirred suspension of $LiAlH_4$ (1.9 g, 0.05 mol) in 100 mL of ether in a flask charged with nitrogen and set up for reflux. After completion of addition the solution was refluxed for 2 h. To the cooled solution, 2 mL of water, 2 mL of 15% aqueous NaOH, and 6 mL of water were added sequentially. The salts were removed by filtration. Removal of the solvent gave a mixture of nonane and the desired amine.

6,6-Dideuterio-1-octylammonium Chloride. The impure amine was dissolved in 25 mL of ether and bubbled with HCl for 15 min.

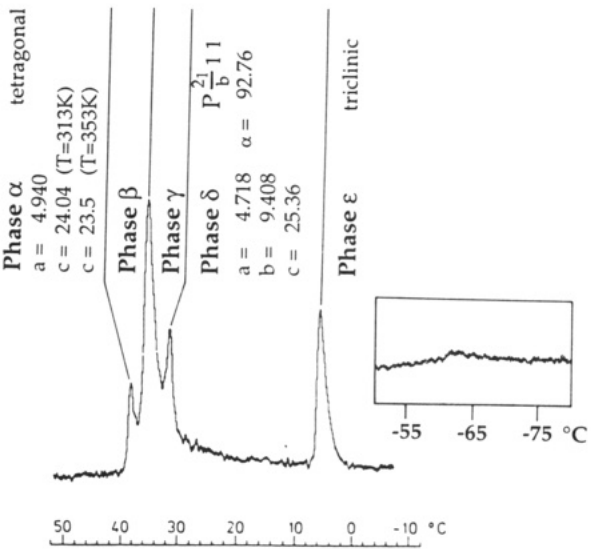

Figure 2. The five solid phases of C8Cl as revealed by dynamical (1 K min^{-1}) DSC. C8Cl had been crystallized, ground, and dried at room temperature prior to the first heating run. Subsequent heating and cooling cycles look exactly like the depicted trace.

A white precipitate formed immediately. The reaction mixture was placed in a freezer overnight. Filtration of the mixture gave the salt (2.1 g), which was rinsed with cold ether and placed in a vacuum desiccator to dry.

Calorimetry. The measurements were performed on a Mettler DSC-30. Prior to the experiments, C8Cl was recrystallized from ethanol at room temperature, ground, and thoroughly dried in a desiccator over P_2O_5. The scanning rate was 1 °C min^{-1}, and the following transition temperatures (K) and enthalpies (kJ mol^{-1}) were observed:

	heating		cooling		
	DSC	Guinier	DSC	Guinier	ΔH
T_{c_1}	278.3		272.9		1.71 (3)
T_{c_2}	304.0	299	302.1	298	
T_{c_3}	307.9	303	306.0	301	4.5
T_{c_4}	310.7	305	309.3	303	

Transition temperatures are reproducible within 0.5 K, transition enthalpies within ±5%. Since our transition enthalpies do not depend on sample history or other experimental conditions as in some other layer compounds,[10,11] we list the measured values. It was impossible to separate (Figure 2) the enthalpies of the $\delta \rightarrow \gamma$, $\gamma \rightarrow \beta$, and $\beta \rightarrow \alpha$ transitions without numerical analysis; since this was not available, we give the combined enthalpies of the three transitions. Our results are in pleasing agreement with an earlier determination.[2]

Crystal Growth. Crystals suitable for X-ray measurements could be grown from a solution of C8Cl in 1-propanol and toluene using a temperature gradient–convection method.[12] They grow in very thin—mostly twinned—flakes which are very sensitive to stress and shear. As an illustration of this fragility, we mention that the space groups of gently treated crystals ($P2_1/b11$) and that of the powders ground from them ($P2_1$ or $P\bar{1}$) are not the same.

Spectroscopy. Raman powder spectra were recorded on a triple monochromator Coderg T800 spectrometer. The 514.5-nm line of a Spectra Physics Model 171 Ar ion laser was used for excitation. A power of up to 250 mW was administered; for some measurements the beam had to be defocalized. The sample temperature was regulated within ±0.5 °C by means of a Coderg CRN2 continuous nitrogen flow cryostat.

Samples for the infrared study were polycrystalline films deposited on CsI windows by rapid evaporation of ethanolic solutions. The spectra were recorded on a Bruker 113v FTIR spectrometer equipped with an MCT detector. The samples were inside a home-built evacuated chamber[13] where temperatures were stable

TABLE I: Crystal Data of $C_8H_{17}NH_3Cl$

	phase δ	phase α
crystal system	monoclinic	tetragonal
a, Å	4.716 (3)	4.940 (8)
b, Å	9.391 (6)	
c, Å	25.38 (2)	24.04 (3)
α, deg	92.65 (5)	
V, Å^3	1123 (2)	587 (2)
Z	4	2
F(000)	368	184
D_c, g cm^{-3}	0.98	0.94
space group	$P2_1/b11$	
μ(Cu Kα), cm^{-1}	25.94	
empirical formula	$C_8H_{20}NCl$	
mol wt, amu	165.71	

within 1 °C. The resolution was 1 cm^{-1}, and 400 scans were accumulated.

Phase Transitions

Inspection of Guinier photographs reveals a delectable agreement with the DSC results. It is quite disturbing, however, that the DSC phase sequence seems to be completely reversible (Figure 2) whereas there exists a minor but conspicuous irreversibility of the phase sequence on the photographs (i.e., phase γ upon heating is different from phase γ′ upon cooling).

A quite unusual behavior should be highlit in Figure 2: in the δ-phase, the heat capacity increases continuously from the ε → δ transition to the onset of the δ → γ transition. The phenomenon causing this rise might be reflected in a gradual decrease of the proton second moment in phase δ.[7]

Another most intriguing thermodynamic feature is displayed in the inset to Figure 2, namely, a very broad, insignificant looking hump at ~210 K. A similar phenomenon has also been observed in the case of C10Cl.[14] It appears tempting to associate this variation of the specific heat with the considerable decrease of the NMR proton second moment ($\Delta M_2 \approx 10$ G^2) observed[7] at ~200 K.

Structural Analysis

Phase ε. Not much is known about this phase (stable below ~273 K). Its powder diagram suggests similarity to phase δ. The larger number of lines (indicating a lower symmetry) and especially their widths prevented, however, a successful indexation of the powder diagram. The structure of phase ε must be very similar to that of phase δ, except that the chains might relax to a more compact packing arrangement.

Phase δ. Single crystals of C8Cl always displayed {100}, {010}, and {001} pinacoids; but only the {001} ones develop neat faces. The very thin (the ratio of width to thickness was ~20) square platelets gave rise to absorption factors between 1.06 and 2.18. Crystal system and space group were determined from precession photographs and the cell constants by centering a few reflections on a Syntex $P2_1$ diffractometer (Table I). Single-crystal X-ray-intensities were measured up to $\sin\theta/\lambda = 0.38$. There resulted 489 reflections of which 216 were considered as unobserved (smaller than 3 esd). The agreement factor between equivalent reflections was a respectable 0.06.

The structure of phase δ[8] (Figures 3 and 4) was determined in space group $P2_1/b11$, by means of the Patterson method, which yielded the chlorine and nitrogen atoms. A Fourier map phased with these atoms revealed only the first carbon atom of the chain. As further Fourier maps did not add to the model, an all-trans chain in the ⟨b,c⟩ plane was tentatively refined. In this refinement, soft constraints[9] on bond distances and angles were imposed. In addition, the root-mean-square vibrational amplitudes along the bonds were forced to comply with the rigid bond criterion.[15] The anisotropic refinement included 425 reflections and 29 soft restrictions; it relied on five observations per parameter and converged to $R_F = 0.127$ and $R_{wR} = 0.04$ (agreement factor of soft restrictions). The largest residue in a final difference Fourier map was smaller than 0.6 e Å^{-3}. The resulting atomic coordinates are listed in Table II.

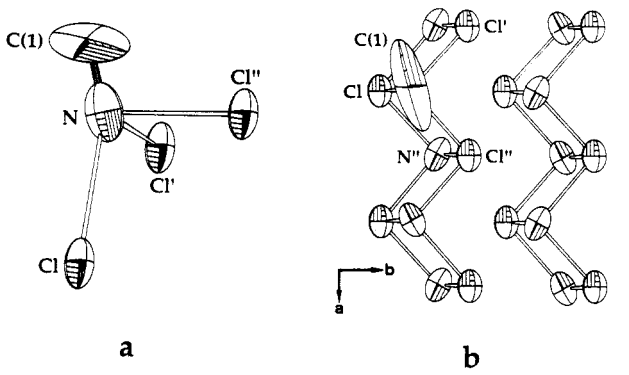

Figure 3. N,Cl partial structure of phase δ of C8Cl. (a) Closeup of the ammonium group. (b) ⟨a,b⟩ projection. Hydrogen bonds are represented by means of double lines.

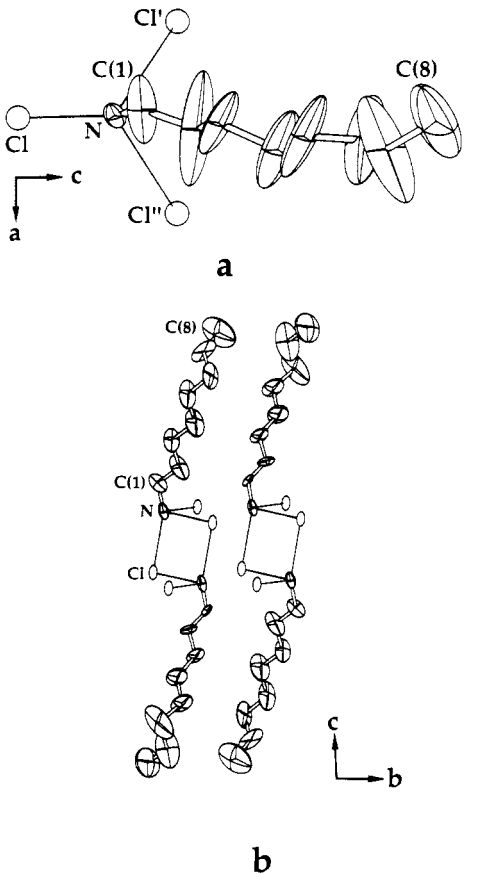

Figure 4. Idealized ⟨a,c⟩ projection (a) and ⟨b,c⟩ projection (b) of phase δ of C8Cl. The idealization consists in several chain conformers being squeezed into one chain in the all-trans conformation. In reality, only 30% of the chains adopt a T_6 conformation.

TABLE II: Atomic Coordinates and Equivalent Displacement Parameters of C8Cl

atom	x	y	z	U_{eq}[a]
Cl	0.744 (3)	0.1088 (5)	−0.0578 (2)	0.091 (3)
N	0.733 (8)	0.157 (2)	0.0689 (8)	0.118 (9)
C(1)	0.70 (1)	0.122 (3)	0.127 (1)	0.32 (4)
C(2)	0.80 (2)	0.230 (4)	0.161 (1)	0.8 (1)
C(3)	0.77 (1)	0.183 (3)	0.217 (1)	0.33 (4)
C(4)	0.91 (1)	0.298 (5)	0.255 (2)	0.50 (6)
C(5)	0.84 (2)	0.258 (4)	0.313 (2)	0.54 (7)
C(6)	0.86 (2)	0.383 (5)	0.350 (2)	0.71 (9)
C(7)	0.91 (2)	0.336 (6)	0.404 (2)	0.9 (1)
C(8)	0.76 (2)	0.433 (8)	0.436 (2)	0.65 (9)

[a] $U_{eq} = {}^1/_3(\beta_{11}a^2 + \beta_{22}b^2 + \beta_{33}c^2 + 2\beta_{23}\mathbf{b}\cdot\mathbf{c})$.

The *n*-caprylammonium ions are arranged in double layers with their methyl ends nearest to each other (*noninterdigitated* structure). Each nitrogen atom participates in three almost equal

TABLE III: Interatomic Distances (Å) and Angles (deg) in C8Cl

N–Cl	3.23 (2)	Cl–N–Cl^a	89.4 (6)
N–Cl^a	3.20 (3)	Cl–N–Cl^b	88.0 (7)
N–Cl^b	3.28 (3)	Cl^a–N–Cl^b	93.2 (5)

$^a x - {}^1/_2, {}^1/_2 - y, -z$. $^b {}^1/_2 + x, {}^1/_2 - y, -z$.

hydrogen bonds (Table III) and Figure 3a). The hydrogen bonding scheme (Figure 3b) consists of endless chains parallel to the *a* axis. The *n*-octylammonium chains lie in the ⟨*b*,*c*⟩ plane and are perpendicular to the *a* axis. The inclination of ~10–15° with respect to the *b* axis leaves plenty of room (~21 Å^2) for lateral movements of the chains; the atoms may be described, however, as occupying the positions of an entirely extended chain. Nitrogen and chlorine atoms lie on positions very close to the ones of the tetragonal high temperature phase. It is important to note that chlorine and nitrogen atoms linked by the *b*-glide plane are almost equivalent with respect to a translation of ${}^1/_2 b$, which accounts for the pseudotetragonal symmetry of phase δ.

Phases β and γ. Almost no information about these phases is available. This deplorable lack is due to the very narrow temperature interval within which they exist: 3 °C for phase β and 4 °C for phase γ. For this reason no powder diagram of phase β is available that is not infested with lines of the neighboring phases. All we may say is that phase β is closer to phase α than to phases γ, δ, and ε (the *c* lattice constant of β[8] is 24.2 Å). A "pure" powder diagram is available of phase γ, but it could not be indexed because of the limited resolution and short wavelength of the copper radiation used in the experiment. In any case, phase γ is more similar to phases δ and ε than to β and α (the *c* lattice constant of γ[8] is 25.05 Å).

Phase α. The powder diagram of this phase (stable above ~311 K) is very similar to those of phases α[6] and α[10] and can be indexed[16] in an "isomorphous", tetragonal cell (Table I).

Finally, the growth of an *interdigitated* phase (analogous to phase i of C10Cl) at ~250 K should be mentioned. For technical reasons no further study could be accomplished.

Vibrational Analysis

Phase ε. At 193 K, the infrared spectrum (Figure 5) of phase ε shows progression bands characteristic of extended structures; their frequencies are in rather good agreement with the values for an all-trans structure obtained by means of a normal coordinate treatment using the geometrical parameters of C10Cl and the same force field.[1] In the Raman spectrum (Figure 6) the most intense bands correspond to all-trans chains, especially in the spectral domain 1000–1200 cm^{-1}. The frequency of the LAM mode is 261 cm^{-1}. This value is higher than that of *n*-nonadecane (251 cm^{-1}),[17] but the difference is about what is expected for the effect of the hydrogen bonds, as observed for C10Cl.[1] The frequency of the $r_{\parallel}(CH_3)$ vibration, 891 cm^{-1}, is specific of a trans conformation in the vicinity of the methyl group. More precisely, the infrared spectrum of DωC8Cl indicates that there are about 10% of gauche bonds in the vicinity of the methyl group. (The two bands at 656 and 622 cm^{-1} (Figure 7) can—by analogy with C10Cl and the *n*-alkanes—be assigned to the rocking deformation of the CD_2 group amidst a TG/GT or a TT sequence, respectively. Assuming that the intrinsic intensities of these transitions are nearly equal, as in *n*-alkanes,[18] one finds the 10% mentioned above.)

Well-defined diffusion bands appear between 2800 and 3100 cm^{-1}. The low frequencies of $\nu_s(CH_2)$ and $\nu_a(CH_2)$, 2842 and 2877 cm^{-1}, respectively, are consistent with the existence of long trans segments in the chains.[19] The maxima at 2871, 2929, and 2961 cm^{-1} correspond to methyl vibrations; the remaining ones are caused by Fermi resonance between $\nu_s(CH_2)$ and the bending progression band overtones.[20] In the $\delta(CH_2)$ spectral domain, the band at 1422 cm^{-1} is a component of the factor group splitting perturbed by Fermi resonance; the other component, near 1445 cm^{-1}, is accompanied by several maxima due to Fermi resonances with overtones and combinations of $r(CH_2)$ transitions.[21,22]

Other factor group splittings are observed, mainly in the infrared spectrum, e.g., of the $r(CH_2)$ mode near 725 cm^{-1} and the asymmetric NH_3 deformation near 1585 cm^{-1}.

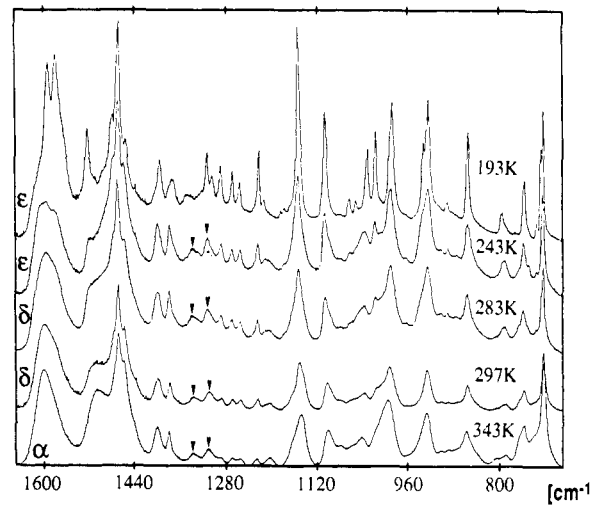

Figure 5. Infrared spectra from C8Cl between 1650 and 700 cm^{-1}. The arrows indicate absorptions assigned to end G forms (at 1340 cm^{-1}) and GTG′/GTG kinks (at ~1310 cm^{-1}).

The position and splitting of the $\delta_a(NH_3)$ deformation and the $\nu_s(NH_3)$ frequency are exactly the same as in phase ε[10]. This correspondence indicates a similar NH_3 fixation to the chlorine matrix in phases ε[8] and ε[10]. The three NH bonds are nearly equivalent.[1]

When the temperature is raised within phase ε, important modifications of the spectra begin to appear. Absorptions corresponding to specific sequences, GTG or GTG′ conformations (near 1310 cm^{-1} and a shoulder at 1368 cm^{-1}) and end G forms, are observed. The intensity of the $r(CD_2)$ band at 656 cm^{-1} progressively increases and corresponds to about 30% of gauche forms in the vicinity of the methyl group at 273 K. The LAM frequency is slightly shifted to 262 cm^{-1}, and its width increases from 8 cm^{-1} at 193 K to 12 cm^{-1} at 258 K; this broadening indicates the presence of several conformers. However, the progression bands are still the dominant features of the infrared spectrum, and the most intense Raman bands are the limiting modes of an infinite trans chain.

Correlation field splittings progressively weaken upon approaching the transition: at 263 K, the $\delta(CH_2)$ component near 1420 cm^{-1} is a weak shoulder of the 1440-cm^{-1} diffusion. The other factor group splittings are no longer observed.

Despite some end gauche defects, phase ε[8] is an ordered crystal with mainly all-trans chains and strong intermolecular interactions at 80 K. The fixation of the NH_3 group to the chlorine matrix is the same as in phase ε[10]. At higher temperature, the weakening of the intermolecular interactions and the existence of a noticeable conformational disorder indicate a great mobility and/or loose packing of the chains.

Phase ε[8] is very similar to the noninterdigitated phase ε[10]. It would probably tend[1] to adopt a denser packing comparable to that of the interdigitated phase i[10], if it were allowed to stay for a long time at a temperature about 25 °C lower than $T_{\delta\rightarrow\epsilon}$.

Phase δ. The factor group is isomorphous to point group $2/m(C_{2h})$, and the number of molecular entities in the unit cell is four. As the symmetry of the molecular sites is 1 (C_1), each of the 81 internal vibrations of the *n*-caprylammonium cation gives rise to a component in each symmetry species of point group C_{2h}. Vibrational modes belonging to the A_g and B_g species are Raman active, and those belonging to the A_u and B_u species are IR active. The geometry of the chain is changing and cannot be specified.

The ε → δ transition causes considerable changes in the spectra; they can be summarized as follows: (i) an increase of the conformational disorder; (ii) the vanishing of all correlation field splittings.

(i) The number of gauche forms in this phase is superior to that of phase ε. In the Raman spectrum, particularly in the CH stretching region, there arise changes analogous to those occurring during the melting of *n*-paraffines:[20] the $\nu_a(CH_2)$ peak height near

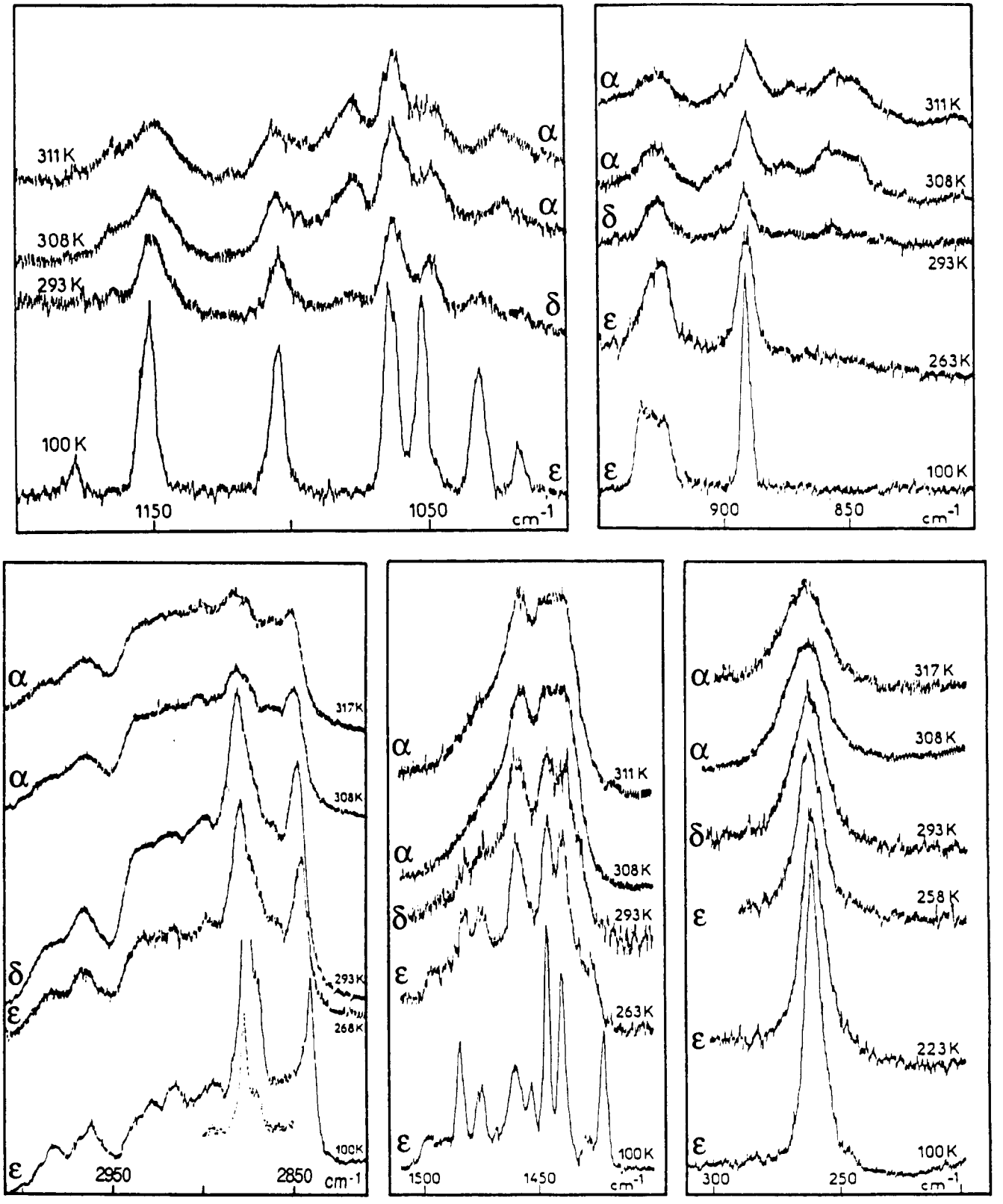

Figure 6. Raman spectra of the various phases of C8Cl.

2880 cm^{-1} decreases, the intensity ratio I_{2937}/I_{2850}, related to the evolution of the gauche bond content, increases, and the $\nu_s(CH_2)$ frequency (near 2850 cm^{-1}) shifts slightly upward (typical of a reduction in the size of the trans sequences).[19] The ($k = 0$ and $k = \pi$) transitions between 1000 and 1200 cm^{-1} are less intense and a signal at 1078 cm^{-1}, characteristic of gauche forms, appears. The DLAM frequency is 263 cm^{-1} (roughly the value of liquid *n*-nonadecane) and its width is about 15 cm^{-1} (indicative of the presence of an increased number of conformers).

The infrared spectrum completes this description; progression bands are less intense and absorptions characteristic of end gauche bonds and GTG′ or GTG sequences are clearly observed. But since the chains have been shown to be approximately parallel and to lie in the ⟨*b*,*c*⟩ plane, only GTG′ sequences (kinks) are allowed. The percentage of gauche bonds in the vicinity of the methyl group, estimated from the spectrum of DωC8Cl, is about 30%. GG defects have not been observed within the accuracy of our experiments.

(ii) Splittings due to the crystalline correlation field have disappeared, in relation with a weakening of the intermolecular interactions. The frequencies of the NH_3 deformations are the same as in phase ϵ.

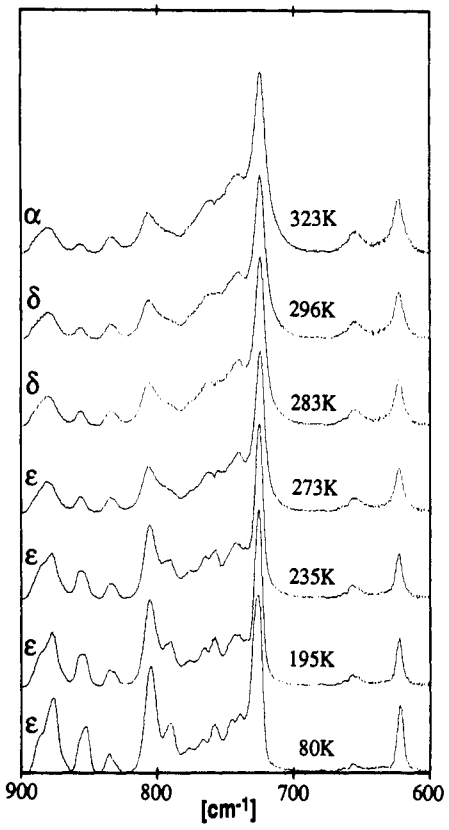

Figure 7. Infrared spectra from the bideuterated derivative DωC8Cl.

Phase δ is thus characterized by an important conformational disorder involving gauche forms and kink defects. These GTG′ sequences allow the chain axes to remain parallel. Intermolecular interactions are weak. The environment of the NH_3 group is roughly the same as in phase ϵ.

Phase α. The conformational disorder increases even more during the $\delta \rightarrow \alpha$ transition. In the Raman spectrum, the bands characteristic of extended structures collapse. The DLAM width reaches 20 cm^{-1}, evidence of a still increasing number of conformers. In the CH stretching domain, the $\nu_a(CH_2)$ band hardly emerges from a broad background; the peak ratio I_{2937}/I_{2850} is strongly enhanced. The diffusion at 1078 cm^{-1} becomes more intense than the bands assigned to the skeleton vibrations of the trans chains. All these features indicate a greater number of gauche defects. This conclusion is confirmed by the infrared spectrum in which the peaks characteristic of extended geometries are replaced by broader bands corresponding to the transitions of several conformers with gauche bonds. No GG defects have been detected, but specific absorptions of GTG or GTG′ sequences and end-G forms are intense; the latter are estimated to about 33% from the integrated intensities of the $r(CD_2)$ transitions.

No Davidov splitting is observed in phase α. The frequencies of the NH_3 deformation bands are nearly the same as in the other phases; the environment of the polar group is therefore not perturbed in any noticeable way at the $\delta \rightarrow \alpha$ transition.

In phase α, the chains do not interact in any appreciable way. They contain GTG′ and GTG sequences and about 33% of their methyl ends are rotated by 120° with respect to the planar trans structure.

There exists a noteworthy difference between the Raman spectra of phases α[8] and α[10] about 15 °C above the $\delta \rightarrow \alpha$ transition. Indeed, a broad and still rather sharp DLAM mode persists in C8Cl, whereas it is well-nigh flattened out in C10Cl.

Conclusions

The description of the disordered phases of C8Cl below is the quintessence of the joint efforts of X-ray diffraction and vibrational spectroscopy.

Phase α, stable above 311 K, represents a state of matter that resembles a *smectic* H, since only chlorine and nitrogen atoms occupy positions of a tetragonal lattice. The carbon atoms of the *n*-octylammonium ion must be disordered. In view of a DLAM width of ~20 cm^{-1}, typical of many different conformers and of a great number of G forms, it seems reasonable to assume that phase α may also be depicted by the turning crankshaft model proposed for C10Cl.[1] This hypothesis is furthermore backed by the absence of GG sequences and a ^1H NMR second moment[7] of 2 G.[2] One should note, however, that in the corresponding phase of C10Cl, the DLAM is completely collapsed: there seem to exist some minor differences in the degree of disorder in phases α[8] and α[10].

Phase δ was available as a single crystal. Although of rather moderate quality it provided plenty of crucial information that was most usefully complemented by spectroscopic results. Again, only chlorine and nitrogen atoms occupy the positions of a lattice (Figure 3a). The chlorine–nitrogen partial structure derives its stability from the N–H···Cl hydrogen bonds; these form endless chains along the *a* axis that may be classified as $C_3^3(4)$ according to Kuleshova and Zorky.[23] It would be most revealing to measure the dielectric tensor in a single crystal in order to corroborate this quite special hydrogen bonding scheme; but this experiment is bound to fail in view of the extremely fragile nature of these crystals. The carbon atoms are *dynamically* disordered as revealed by a ^1H NMR second moment[7] of 5 G,[2] the lack of correlation field splittings, a DLAM width of ~15 cm^{-1}, and the high number of GTG and GTG′ sequences. Only an average chain could be refined under these circumstances, by imposing distance and angle constraints (Figure 3). The excessive (root-mean-square displacement ≈1.5 Å along the *a* axis) probability ellipsoids of Figure 3b may be interpreted as caused by the superposition of several conformers. The elongated ellipsoids are exactly what one would expect for different kinks at a given position in the chains. Of course, this study does not reveal anything about the time regime of the kinks: whether we have several static kinks or kink diffusion; but a recent INS study[29] of the similar layer compound $(n\text{-}C_{10}H_{21}NH_3)_2MnCl_4$ seems to be in favor of several static kinks. Considering the *c* lattice constant, it appears safe, moreover, to rule out more than one kink (GTG′) sequence.

Phase ϵ represents a crystallographic nightmare: no single crystals, triclinic symmetry, and broad, fuzzy powder lines that cannot be indexed reliably. Indeed, a synchrotron radiation of ~3–5 Å might provide the resolution necessary to index this phase. Fortunately, vibrational spectroscopy furnishes plenty of decisive information on the chains. All seems to indicate entirely extended chains, at least at liquid nitrogen temperature (except for a few end G forms). It is interesting to note that upon warming up, still inside phase ϵ, defects such as end-G forms (Figure 5) are gradually introduced into the chains.

The results of the present investigation combined with previous NQR[4] and NMR studies can now be woven into the following picture of the four thermotropic phase transitions in the C8Cl system.

The elusive $\alpha \rightarrow \beta$ transition manifests clearly in calorimetry (Figure 2) and on powder photographs. It is not at all obvious what the small transition enthalpy is used for; for ^{35}Cl and ^{14}N NQR spectra,[5,6] IR spectra (Figures 5 and 7) and the d_{00l} distances are very similar indeed in both adjacent phases. Yet the powder diagrams are different. The difference may consist in a symmetry reduction from tetragonal to orthorhombic. This hypothesis is founded on a group theoretical analysis[25] and a ^2H NMR study[26] of C10Cl. Indeed, different line shapes and spin–lattice relaxation times could be observed for phase β[10]. The available data are compatible with space group *Pmmm* for phase β[8]. Our model of this transition could then look like this: Upon passing the $\alpha \rightarrow \beta$ transition temperature, some lattice mode changes and the symmetry of the chlorine cavity is reduce from *4mm* to *2mm*. As a consequence, the dynamics of the *n*-caprylammonium chains change, too: from a three-site jump to a two-site disorder. It should be noted, however, that the chains are likely to remain in a state with every other C–C bond vertical, as may be concluded from the invariance of the d_{00l}.

The $\beta \rightarrow \gamma$ transition consumes the major part of the enthalpy. The d_{00l} interlayer distance increases by 1 Å during this transition. The powder diagram of phase γ resembles much the one of phase δ. Since the chains have been shown to be nearly extended in phase δ[8], they are likely to be nearly extended in phase γ[8] as well, and we may conclude that the energy is mainly used to uncurl the chains (from the partially coiled up state in phase β to the essentially extended state in phase γ). This reversion of the chain melting results in the observed increase of 1 Å in the basal spacing d_{00l}. The uncoiling of the chains also brings about a further distortion of the chlorine cavity after which the ammonium group is locked into one position.

During the $\gamma \rightarrow \delta$ transition the chains acquire a more compact packing. The transition can be understood by regarding the chains as cylinders of electron density sliding into positions of lesser energy. This denser packing results in a doubling of the b axis.

In the $\delta \rightarrow \epsilon$ transition finally, the chains relax into an even more compact packing and two formerly equivalent ammonium groups differentiate. But even phase ϵ is not a stable phase yet; chain interdigitation is likely to occur within days or under a small pressure. If cooled down right after the transition, the phase does not undergo any further transition but changes nevertheless quite radically between room and liquid nitrogen temperatures (gradual loss of G forms; see Figure 7).

In general, two features ought to be emphasized: first, not all measurable quantities manifest changes at all phase transitions (e.g. IR/Raman spectra above 200 cm^{-1} do not display abrupt changes at these first-order phase transitions. Secondly, some observables vary in quite a gradual manner as if completely ignoring the phase transitions (e.g., the width of the LAM-1 seems to continuously increase from liquid nitrogen temperature up to 330 K (Figure 6)). A similar behavior has also been observed in C14Mn.[24]

The number and frequencies of ^{14}N and ^{35}Cl NQR lines belong to those features that change discontinuously. The changes are caused by symmetry changes of the chlorine cavity in which the NH_3 polar heads are embedded. These symmetries are broken exactly at the critical temperatures listed in Table 1; part of the transition enthalpies must therefore be consumed by them. As mentioned above, the lattice constants provide another example of an abruptly changing quantity.

Percentages of G forms and kinks (GTG′ sequences) increase continuously from liquid nitrogen temperature upward. An opposite but also continuous trend is observed for the factor group splitting. Actually, no discontinuous behavior can be detected in connection with the chains, although the ^1H NMR second moment[7] changes somewhat abruptly at the critical temperatures. Even the b lattice constant doubling does not entail any discontinuities although the chains seem to be the cause rather than the consequence of the doubling.

The combination of several physical methods has brought forth quite detailed mechanisms of the phase transition in C8Cl. The close resemblance of its phases with smectic mesophases observed in cell membranes might eventually lead to a deeper understanding of the much more complex real systems. This hope appears indeed justified in the light of quite a few analogies between C8Cl and biomembranes: (i) the *thickness of the bilayers* decreases with the temperature (by 10% in C8Cl, versus 20% in the erucate-enriched membranes of *Acholeplasma laidlawii*[27]); (ii) the *area per chain* increases with temperature (by 15% in C8Cl versus 50% in the membranes[27]); (iii) there exists a *chain interdigitation transition* (transforming a bilayer into an interdigitated monolayer (observed under the influence of polymyxin B, acetylcholine, or choline in DPPC[28] and as a thermotropic phase transition in C8Cl). The results of this investigation and an analogous study of C10Cl,[1] as well as forthcoming INS[29] and NMR[26] results, could then be used as a powerful starting point for a molecular modeling study of the phase transition in biomembranes.[30]

Acknowledgment. We heartily thank Judit Miklossy for reading the manuscript and for constructive criticism. Georges Burri's kind preparation of the electron micrograph is sincerely appreciated.

Registry No. C8Cl, 142-95-0.

References and Notes

(1) Schenk, K. J.; Ogle, C. A.; Chapuis, G.; Cavagnat, R.; Jokic, A.; Rey-Lafon, M. *J. Phys. Chem.* **1989**, *93*, 5040.
(2) Tsau, J.; Gilson, D. F. R. *J. Phys. Chem.* **1968**, *72*, 4082.
(3) Busico, V.; Scopa, A.; Vacatello, M. *Z. Naturforsch.* **1982**, *37a*, 1466.
(4) Busico, V.; Cernicchiaro, P.; Corradini, P.; Vacatello, M. *J. Phys. Chem.* **1983**, *87*, 1631.
(5) Seliger, J.; Žagar, V.; Blinc, R.; Kind, R.; Arend, H.; Milia, F. *Z. Phys. B* **1987**, *67*, 363.
(6) Seliger, J.; Žagar, V.; Blinc, R.; Kind, R.; Arend, H.; Chapuis, G.; Schenk, K. J.; Milia, F. *Z. Phys. B* **1987**, *69*, 379.
(7) Tsau, J.; Gilson, D. F. R. *Can. J. Chem.* **1973**, *51*, 1990.
(8) Kind, R.; Blinc, R.; Arend, H.; Muralt, P.; Slak, J.; Chapuis, G.; Schenk, K. J.; Žekš, B. *Phys. Rev.* **1982**, *A26*, 1816.
(9) Waser, J. *Acta Crystallogr.* **1963**, *16*, 1091. Bärlocher, Chr.; Hepp, A.; Meyer, W. M. DLS-76—Program Description, ETH Zürich, 1976.
(10) Schenk, K. J.; Chapuis, G. *J. Phys. Chem.* **1988**, *92*, 7141.
(11) Needham, G. F.; Willett, R. D.; Franzen, H. F. *J. Phys. Chem.* **1984**, *88*, 674.
(12) Arend, H., private communication.
(13) Cornut, J. C.; Huong, P. V.; Graja, A.; Daleau, G. *Appl. Spectrosc.* **1988**, *8*, 1401.
(14) Chanh, N. B.; Housty, J. R., private communication.
(15) Hishfeld, F. L. *Acta Crystallogr.* **1976**, *A32*, 239. Hazel, M.; Hishfeld, F. L. *Acta Crystallogr.* **1975**, *B31*, 162.
(16) Taupin, D. Powder Diagram Indexing Routine, Version 1974, based on: Taupin, D. *J. Appl. Crystallogr.* **1968**, *1*, 178.
(17) Scherer, J. R.; Snyder, R. G. *J. Chem. Phys.* **1980**, *72*, 5798.
(18) Snyder, R. G.; Maroncelli, M.; Strauss, H. L.; Elliger, L. A.; Cameron, D. G.; Casal, H. L.; Mantsch, H. H. *J. Am. Chem. Soc.* **1983**, *105*, 133.
(19) Ricard, L.; Abbate, S.; Zerbi, G. *J. Phys. Chem.* **1985**, *89*, 4793.
(20) Synder, R. G.; Scherer, J. R. *J. Chem. Phys.* **1979**, *71*, 3221.
(21) Abbate, S.; Zerbi, G.; Wunder, S. C. *J. Phys. Chem.* **1982**, *86*, 3140.
(22) Snyder, R. G.; Hsu, S. L.; Krimm, S. *Spectrochim. Acta* **1978**, *34A*, 395.
(23) Kuleshova, L. N.; Zorky, P. M. *Acta Crystallogr.* **1980**, *B36*, 2113.
(24) Almirante, C.; Minoni, G.; Zerbi, G. *J. Phys. Chem.* **1986**, *90*, 852.
(25) Kind, R., private communication.
(26) Schenk, K. J., et al., to be published.
(27) Engelman, D. M. *J. Mol. Biol.* **1971**, *58*, 153.
(28) Ranck, J. L.; Tocanne, J. F. *FEBS Lett.* **1982**, *143*, 175.
(29) Rey-Lafon, M., et al., to be published.
(30) Vacatello, M.; Busico, V. *Mol. Cryst. Liq. Cryst.* **1984**, *107*, 341.